Multi-wavelength studies of the broad line radio galaxies IGR J21247+5058 and 3C 390.3

C. Ricci[*ab], **V. Beckmann**[ab], **T. J.-L. Courvoisier**[ab], **M. Audard**[a]b **and P. Lubiński**[ac]

[a] *ISDC Data Centre for Astrophysics, 1290 Versoix, Switzerland*
[b] *Observatoire Astronomique de l'Université de Genève, 1290 Sauverny, Switzerland*
[c] *Centrum Astronomiczne im. M. Kopernika, PL-00-716 Warszawa, Poland*
E-mail: `Claudio.Ricci@unige.ch`

We present a multi-wavelength study of two broad line radio galaxies: IGR J21247+5058, one of the brightest AGN discovered by INTEGRAL, and 3C 390.3, also extensively observed by INTEGRAL. All the available INTEGRAL, XMM-Newton and Swift data were analysed, covering the 0.3–200 keV range. The spectral energy distribution of IGR J21247+5058 was extracted from the total observed spectrum in the IR to UV bands, using a blackbody model to account for the emission of a star in the line of sight. The broad band X-ray spectrum of IGR J21247+5058 can be described by a cut-off ($E_C = 206^{+180}_{-61}$ keV) power law ($\Gamma = 1.56^{+0.09}_{-0.07}$) plus a reflection component ($R = 0.8^{+0.5}_{-0.4}$), absorbed by a double layer of partially covering neutral material. The X-ray spectrum of 3C 390.3 can be represented by an absorbed power law ($N_H \simeq 4.5 \times 10^{20}$ cm^{-2}, $\Gamma = 1.78^{+0.02}_{-0.02}$) plus a blackbody component ($kT \simeq 150$ eV). Both radio galaxies show weak Kα iron lines. The spectral energy distribution of IGR J21247+5058 shows the presence of two peaks, one in the near infrared and one in the X-rays. While the X-ray peak may be due to inverse Comptonisation of synchrotron photons, the one in the IR is likely due to thermal emission. The spectral energy distribution of 3C 390.3 shows two strong peaks in the IR and X-rays and a third peak in the UV, whose height varies considerably between XMM-Newton and Swift observations. The IR peak is interpreted as due to synchrotron emission, while the one in the UV as emission from the disk, and it does not seem to be related to the soft excess in the X-rays.

---

[*]Speaker.

1. Introduction

Radio galaxies are active galactic nuclei (AGN) with regions of synchrotron-emitting plasma that can extend to thousands of kiloparsecs. They are thought to be powered by narrow collimated jets, which seem to originate directly from the central engine, terminating in high surface brightness regions called *hot spots*. The jets show polarized emission and non-thermal continua, and thus are thought to result from synchrotron emission. Radio galaxies are divided, according to the width of their optical emission lines, into broad line radio galaxies (BLRG) and narrow line radio galaxies (NLRG). According to the unified scheme for radio-loud AGN (Antonucci 1993; Urry & Padovani 1995), radio galaxies, radio loud quasars and blazars are the same physical objects seen at decreasing angles with respect to the jet axis. The X-ray spectra of this class of objects present different characteristics than their radio-quiet counterparts, the Seyfert galaxies. Indeed while the presence of Compton reflection is prominent in the spectra of Seyfert galaxies above 10 keV (Pounds et al. 1989), it is weak or absent in the case of BLRG (Zdziarski et al. 1995, Wozniak et al. 1998). Another effect of reflection of the primary X-ray radiation on the disk, the Fe Kα line, is weaker in the spectra of BLRG than in Seyfert galaxies (Wozniak et al. 1998). The multi-wavelength spectral energy distribution (SED) of radio galaxies is consistent with the double peaked shape observed in BL Lacs (Trussoni et al. 2003). The two peaks, in the IR (or far IR) and γ-rays, are usually interpreted (Ghisellini et al. 1998) as due to synchrotron radiation of relativistic electrons from the jet, and to inverse Compton scattering of synchrotron photons (SSC model) or of thermal photons originated in the disk, in the broad line region (BLR) or in the torus (EC model).

Among the 50 new sources detected by *INTEGRAL* and identified as AGN, the brightest in the 20–40 keV band is IGR J21247+5058, with a flux of $F_{20-40\,\mathrm{keV}} = (4.2 \pm 0.4) \times 10^{-11}$ ergs cm^{-2} s^{-1} (Beckmann et al. 2006). Optical observations show the presence of a star in the line of sight of IGR J21247+5058, which strongly contaminates the optical data (Masetti et al. 2004). Recently IGR J21247+5058 has been classified as an intermediate FR I/FR II Broad Line Radio Galaxy with characteristics similar to 3C 390.3 (Molina et al. 2007).

3C 390.3 is a luminous ($L_{(2-10\mathrm{keV})} \sim 3 \times 10^{44}$ ergs s^{-1}) nearby (z=0.057) broad line FR II radio galaxy detected for the first time in the X-rays by *OSO 7* (Mushotzky, Baity, & Peterson 1977). The spectrum of this object in the 0.5–8 keV band has been described by an absorbed power law (Eracleous, Halpern, & Livio 1996 using *ASCA*/SIS data) with a photon index of $\Gamma = 1.68^{+0.04}_{-0.04}$ and an intrinsic hydrogen column density $N_H = (4.6^{+1.5}_{-1.5}) \times 10^{20}$ cm^{-2}. The presence of an iron Kα line at 6.4 keV (in the rest frame of the source) with an equivalent width of EW$= 190^{+100}_{-70}$ eV has also been reported using *ASCA* data (Eracleous, Halpern, & Livio 1996). Using *BeppoSAX* data Grandi et al. (1999) found evidence of a reflection component ($R = 0.9^{+0.5}_{-0.3}$) in the spectrum of 3C 390.3.

2. The high-energy emission of IGR J21247+5058 and 3C 390.3

The set of data used for the *INTEGRAL* spectrum of IGR J21247+5058 includes all the public data available (as of January 2008) plus private data taken in December 2007 (P.I. Beckmann), for a total exposure time of about 2.6 Ms. The use of OSA 7 and the additional set of data allowed us to extract a spectrum with higher resolution and up to higher energies ($\sim$ 210 keV) than the

one previously reported in the literature (Molina et al. 2007). At lower energies we used *XMM-Newton* and *Swift* data, previously analyzed by Molina et al. (2007) and Malizia et al. (2007). The high-energy (0.3–212 keV) spectrum of IGR J21247+5058 can be well described ($\chi^2_\nu = 1.07$) by a power law ($\Gamma = 1.56^{+0.09}_{-0.07}$) plus a reflection component from neutral material ($R = 0.8^{+0.5}_{-0.4}$). For the absorption we used Galactic absorption plus two layers of partially absorbing material, as proposed by Molina et al. (2007). This phenomenological model provides a good description of a scenario involving a hot corona emitting medium-hard X-rays by Comptonisation of seed photons emitted by synchrotron emission from a jet or by an accretion disk (Haardt & Maraschi 1991) plus a reflection component from a disk. Evidence of a soft excess is seen in *XMM-Newton* data, but due to the strong Galactic absorption it is impossible to study it accurately. There is no significant evidence of an iron Kα line in the spectrum of IGR J21247+5058, with a 40 eV upper limit (3σ) on the equivalent width. The luminosity of IGR J21247+5058 in the 0.1–200 keV band is $L_{0.1-200\,keV} = (2.1 \pm 0.1) \times 10^{44}\,erg\,s^{-1}$

For comparison we analysed the well-known broad line radio galaxy 3C 390.3, whose luminosity is $L_{0.1-200\,keV} = (1.3 \pm 0.1) \times 10^{45}\,erg\,s^{-1}$. *INTEGRAL* data for a total exposure time of 346 ks are available for 3C 390.3, while at lower energies the source has been observed twice in a time span of 8 days by *XMM-Newton*, and once by *Swift*/XRT. The overall high-energy spectrum of 3C 390.3 (in the 0.3–200 keV band) presents a power-law like continuum plus a soft excess, which has been fitted using a blackbody component at low energies ($E < 1$ keV), and an iron Kα line at 6.4 keV (in the rest frame of the source). Combining IBIS/ISGRI and EPIC/PN data of 3C 390.3 we obtained an intrinsic absorption of $N_H^{intr.} \simeq 3 \times 10^{19}\,cm^{-2}$, a photon index of $\Gamma = 1.78^{+0.02}_{-0.02}$, a temperature of the blackbody component of $kT = 146^{+10}_{-8}$ eV ($\chi^2_\nu = 1.03$) and an equivalent width of the Kα line of about 50 eV. Combining XRT and IBIS/ISGRI data we obtained values consistent with those obtained using PN. The presence of the soft excess below 1 keV has previously only been detected by Ghosh and Soundararajaperumal (1991) using *EXOSAT* data and by Molina et al. (2008) using *XMM-Newton* data, while further observations did not confirm the existence of this feature.

The main differences between the X-ray spectra of these two AGN are the following: 3C 390.3 presents a stronger iron Kα line ($EW \simeq 50$ eV) than IGR J21247+5058, for which only a 3σ upper limit EW< 40 eV can be determined, and the continuum of 3C 390.3 does not show evidence of a cut-off or of a reflection component. Consistent with the weak iron Kα line in 3C 390.3 is the fact that a reflection hump is weak or not detectable. The iron Kα line of 3C 390.3 is weaker than what was previously found by Grandi et al. (1999). The equivalent widths of the iron Kα lines of 3C 390.3 and IGR J21247+5058 are consistent with the average value of $< EW_{BLRG} > = 71 \pm 45$ eV for broad line radio galaxies (Grandi et al. 2002).

It should be noted that beside being curved, the soft continuum of IGR J21247+5058 is flatter than the typical value observed for bright BLRG ($< \Gamma_{BLRG} > \simeq 1.73$, Grandi et al. 2000). The presence of a reflection hump in the spectrum of IGR J21247+5058 is evident only considering a complex absorption model (namely two layers of partially absorbing material), while it is not necessary when using a simple absorption layer. Thus the high-energy spectrum of IGR J21247+5058 should be better investigated when new *INTEGRAL* data will be available, in order to better constrain its spectral features and understand whether reprocessed X-ray emission is important or not. Moreover more accurate data in the soft X-rays would be fundamental to understand the nature of the absorber.
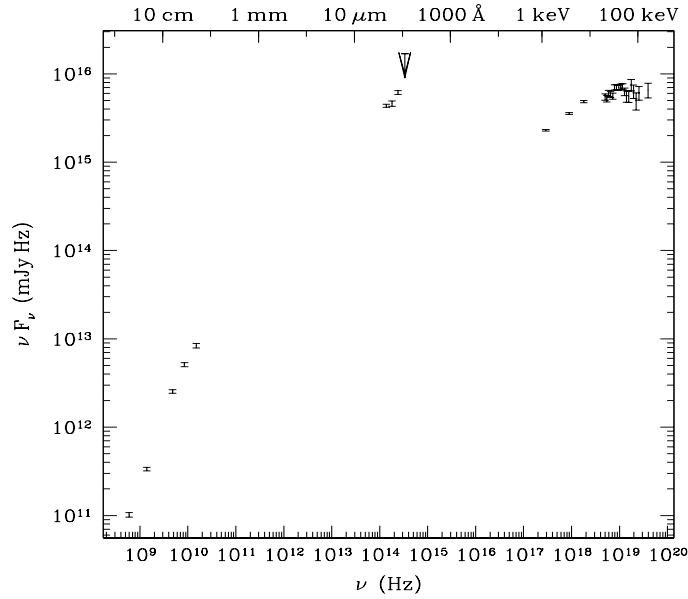
Figure 1: Spectral energy distribution of IGR J21247+5058 corrected for absorption and for the flux of the superimposed star in the K_s, H, J and I bands. In the high energies *INTEGRAL* IBIS/ISGRI and *XMM-Newton* EPIC/MOS data have been used. In the optical the values are those obtained by Loiano's telescope observations (Masetti et al. 2004), in the IR those resulting from 2MASS observations, while in the radio values from VLA and GMRT observations have been used (Molina et al. 2007).

3. The SED of IGR J21247+5058

The SED of IGR J21247+5058 has to be carefully analysed in order to understand the respective contributions of the galaxy and of the star on the line of sight. Indeed from the optical and UV data the presence of a star in the line of sight of IGR J21247+5058 is evident: the spectrum of the optical counterpart of the galaxy shows a continuum and absorption lines typical for an F or G-type star (at z=0) plus a broad feature which has been identified as the Hα emission line of the AGN at z=0.02 (Masetti et al. 2004). While the optical spectrum shows the presence of a star in the line of sight, the near infrared photometry performed by 2MASS is not consistent with a stellar spectrum (Combi et al. 2005). Using a blackbody model (with a temperature of $T = 6000$ K) for the emission of the star we corrected the values in the IR and optical in order to extract the emission of the AGN. Then we corrected the remaining fluxes for absorption.

In Figure 1 the corrected SED of IGR J21247+5058 is shown. The global structure of the corrected spectral energy distribution of IGR J21247+5058 could be interpreted in two different ways:

- We detect two "bumps" at about the same height in the logarithmic νF_ν diagram, one in the near IR and one in the X-rays. This can be attributed to synchrotron emission and inverse Compton-scattering of synchrotron photons for the low frequency ($\sim 10^{15}$ Hz) and high-frequency peak ($\sim 10^{19}$ Hz), respectively. This synchrotron self-Compton model (SSC) is used in the case of radio-loud objects such as blazars and radio galaxies (e.g. Ghisellini et

al. 1996). In the case of the low-energy peak, the absorption due to the Galactic medium and the flux of the star in the line of sight make it impossible to see the expected optical-UV cutoff.

- Another scenario would be that we detect synchrotron emission in the radio but that the IR-UV emission is not arising from the central engine but from thermal emission. The high-energy emission would be again due to the inverse Compton scattering of the synchrotron photons. This hypothesis is supported by the fact that the IR spectrum is not a simple extrapolation of the radio spectrum.

In order to check whether the IR emission comes from synchrotron emission of the AGN we used the SSC model of Ghisellini et al. (1996) for estimating the magnetic field B of the AGN. The magnetic field is given by:

$$B \cdot D = (z+1) \frac{v_S^2}{3.7 \times 10^6 v_C}, \qquad (3.1)$$

where z is the redshift, v_S and v_C are the frequencies of the synchrotron and the inverse Compton peak, respectively, and D is the Doppler factor:

$$D = \frac{1}{\gamma(1 - \beta \cos \theta)}. \qquad (3.2)$$

Assuming a viewing angle of $\theta \simeq 35°$ (Molina et al. 2007) and a Lorentz factor $\gamma = 5$ (Giovannini et al. 2001), we obtain a Doppler factor of $D \simeq 1$. The peak of the inverse Compton branch is located at $v_C \simeq 10^{19}$ Hz, while the peak of the synchrotron emission is less constrained, but we can assign a lower limit of $v_S \gtrsim 10^{14.5}$ Hz. From this we derive an unlikely lower limit for the magnetic field of IGR J21247+5058: $B \gtrsim 3600$ Gauss. This points to an IR emission dominated by thermal emission rather than resulting from non-thermal synchrotron emission of a jet.

Another parameter interesting to study the SSC model of Ghisellini et al. (1996) is the Lorentz factor γ_b of the electrons contributing most to the power output:

$$\gamma_b = \left(\frac{3v_C}{4v_S} \right)^{\frac{1}{2}}. \qquad (3.3)$$

Using the values reported above we obtain a Lorentz factor of $\gamma_b \lesssim 150$. However this value is a rough estimate only, in fact if thermal emission is dominant in the IR we cannot assess correctly the location of the synchrotron peak.

4. The SED of 3C 390.3

The SED of 3C 390.3 (Figure 2) is much better constrained than that of IGR J21247+5058 and shows a similar structure, with a strong emission in the IR (which peaks at $v \simeq 10^{13}$ Hz), which height is comparable to that of the IC component, and a third peak in the optical/UV. The peak of the IC component is not well constrained: $v_C \gtrsim 10^{19}$ Hz. Considering $\theta \simeq 26°$ (Eracleous & Halpern 1994) and $\gamma = 5$ and applying to this SED Eq. (3.1), we obtain an upper limit for the magnetic field of $B \lesssim 1.7$ Gauss. Applying Eq. (3.3) we obtain a lower limit for the energy of
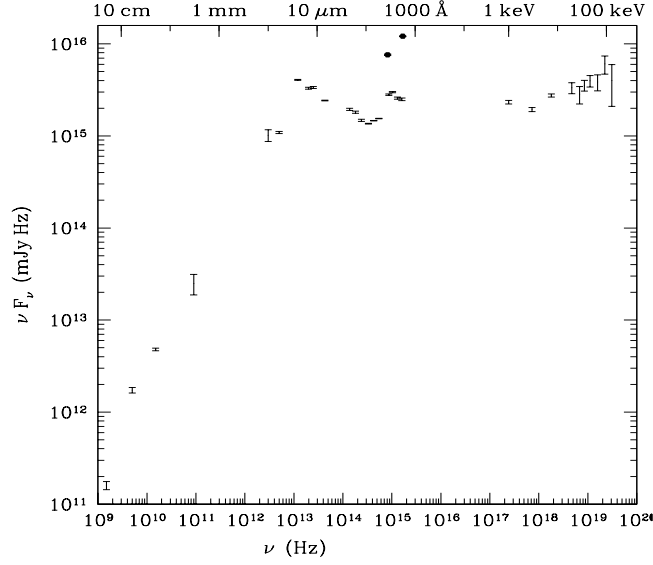
Figure 2: Spectral energy distribution of 3C 390.3 after having corrected for absorption in the X-rays, UV, optical and near IR. The values used in the X and γ-rays are those obtained by *XMM-Newton* EPIC/PN and *INTEGRAL* IBIS/ISGRI. Given the variability of the source, in the optical for the V, R and I bands the data used are the weighted averages of those obtained by the optical monitoring of the source performed by Tao et al. (2008) from 1995 to 2004. In the U, UVW1, UVM2 and UVW2 bands we used *XMM-Newton*/OM values. In the radio domain we used data from Rudnick et al. (1986) and Steppe et al. (1988). In the far IR we used the weighted averages of IRAS data (at 12, 25, 60 and 100μm), in the mid-IR data coming from *Spitzer* (Ogle et al. 2006), while in the near infrared we used 2MASS observations of the source in the J, H and K bands. The circles represent the fluxes in the U and UVW2 bands as measured by Swift/UVOT.

the electrons contributing most to the power output of $\gamma_b \gtrsim 900$. 3C 390.3 shows a strong flux variation in the U and UVW2 bands (Figure 2) during the 31 months between the *Swift*/UVOT and the *XMM-Newton*/OM observations, while over this time span the X-ray flux does not vary significantly. While at the time of *XMM-Newton* observations the UV peak was smaller than those in the IR and X-rays, it was dominant during the *Swift* observation. We registered a variation by a factor of $\simeq 5$ and of $\simeq 3$ in the UVW2 and U band, respectively. Another remarkable difference between the two observations is the spectral slope, which varies by $\Delta\alpha \simeq 0.7$ between $\alpha_{Swift/UVOT} \simeq -0.35$ and $\alpha_{XMM/OM} \simeq -1.04$. The presence of this blue bump was not detected in previous observations (Wamsteker et al. 1997). The amplitude of the UV variability is consistent with what has been found by *IUE* observations of 3C 390.3 performed from 1978 to 1994 (Zheng 1996), but the fluxes observed by *IUE* were significantly lower than those measured by *Swift*. *IUE* observations showed a very strong flux variations in the UV, with a peak at 1350 Å, where a variation by a factor of $\simeq 27$ was registered. At 1850 Å (wavelength very close to the center of the UVW2 band) Zheng (1996) measured a variation by a factor of $\simeq 12$.

The radio spectrum of this AGN is well represented by a simple power law with a energy index $\alpha = -0.75 \pm 0.10$. Using only the flux at 60, 25 and 12 μm (as the flux at 100 μm is subjected to cirrus contamination) the FIR spectrum shows a power law with a spectral index $\alpha = 0.7 \pm 0.2$. We can conclude that the emission of 3C 390.3 is probably due to synchrotron and SSC emis-

sion in the radio-IR and γ-rays respectively, while the optical-UV bump is likely due to the disk. This component could be due either to optically thick emission from the disk or to disk heating by primary X-ray radiation. We measured a strong variability of the optical-UV bump in the 31 months between *XMM-Newton* and *Swift* observations, which is not observed in the soft excess in the X-rays, and which could point to the fact that the processes involved are not the same. This could confirm the hypothesis of Molina et al. (2008) that the soft excess is produced by the extended soft X-ray emission around the nucleus observed in *Chandra* images (Hardcastle & Croston 2004). Regardless of the strong UV variability the X-ray continuum did not show any significant variation in the 31 months between the two observations. This points to the fact that in case UV emission is mainly due to reprocessing of X-ray radiation from the corona, as suggested by Grandi et al. (1999), there could have been a burst in the X-ray emission in the 2.5 years between the two observations. Unfortunately there are no *INTEGRAL* observations available over that period, and there is no evidence of a burst at that time in the *Swift*/XRT observation. Another explanation of this variability could come from instabilities in the disk, as for example discharges of an active magnetic blob above the accretion disk (Haardt et al. 1994). Wamsteker et al. (1997) found that the continuum spectrum from the optical to the X-rays can be described by a single power law with index $\alpha \simeq -0.9$. The results we obtained using *XMM-Newton*/OM and *Swift*/UVOT are different ($\alpha_{Swift/UVOT} \simeq -0.35$ and $\alpha_{XMM/OM} \simeq -1.04$), and in particular the UVOT photon index is much flatter than what was found by Wamsteker et al. (1997).

5. Conclusions

The main difference in the SED of these two radio galaxies is the IR component, which has a peak at higher energies in the case of IGR J21247+5058. This is probably due to the fact that the emission processes at these frequencies are different, thermal emission in the case of IGR J21247+5058 and synchrotron emission for 3C 390.3.

The spectral energy distribution of IGR J21247+5058 shows an IR peak which is located where one would expect it for low-peaked BL Lac (LBL) objects, while the IC peak is located at energies smaller than those normally found for LBL ($\nu_{IC}^{LBL} \sim 10^{21}$ Hz). This could confirm the classification of IGR J21247+5058 as a radio galaxy, with a strong thermal emission in the IR. The identification of IGR J21247+5058 as a Type 1 AGN (Masetti et al. 2004) is based on the identification of one additional spectral feature on the optical spectrum, which is dominated by the foreground star. If the identification of this feature with the Hα line is not correct, then IGR J21247+5058 might still be a member of the BL Lac class, even though the SED seems to discredit this hypothesis, or of the narrow line radio galaxies class. More accurate optical observations of this source are needed in order to resolve it from the foreground star, thus permitting to better understand its nature.

In order to understand the connection between the physical mechanism ruling Seyfert type objects on one side and radio galaxies on the other, it is necessary to increase the number of objects with reliable SEDs. IGR J21247+5058 and 3C 390.3 are two examples that show the importance of detecting additional strong X-ray emitting radio galaxies, in order to bridge this gap. Thus, *INTEGRAL* and *Swift* provide excellent tools in order to identify radio galaxies and, together with observations in the IR and optical, to create a significant sample of X-ray bright radio galaxies.

Antonucci, R. R. J. 1993, ARA&A, 31, 473

Beckmann, V., Soldi, S., Shrader, C. R., et al. 2006, ApJ, 652, 126

Combi, J. A., Ribo, M., Mirabel, I. F. 2005, Ap&SS, 297, L385

Eracleous, M., Halpern, J. P. 1994, ApJS, 90,

Eracleous, M., Halpern, J. P., Livio, M. 1996, ApJ, 459, 891

Ghisellini, G., Maraschi, L., Treves, A., Tanzi, E. G. 1986, ApJ, 310, 317

Ghisellini, G., Maraschi, L., Dondi, L. 1996, A&AS, 120, 503

Ghisellini, G., Celotti, A., Fossati, G., et al. 1998, MNRAS, 301, 451

Ghosh, K. K. & Soundararajaperumal, S. 1991, AJ, 102, 1298

Giovannini, G., Cotton, W. D., Feretti, L., Lara, L., Venturi, T. 2001, ApJ, 522, L97

Grandi, P., Guainazzi, M., Haardt, F., et al. 1999, A&A, 343, 33

Grandi, P., Palumbo, G. G. C., Giommi, P., et al. 2000, AIPC, 510, 382

Grandi, P., Urry, C. M., Maraschi, L. 2002, NewAR, 46, 221

Haardt F. & Maraschi L. 1991, ApJ, 380, L51

Haardt F., Maraschi L., Ghisellini, G. 1994, ApJ, 432, L95

Hardcastle, M. J., & Croston, J. H. 2005, MNRAS, 363, 649

Kruper, J. S., Urry, C. M., Canizares, C. R. 1991, ApJS, 74, 347

Malizia, A., Landi, R., Bassani, L., et al. 2007, ApJ, 668, 81

Masetti, N., Palazzi, E., Bassani, L., et al. 2004, A&A, 426, L41

Molina, M., Giroletti, M., Malizia, A., et al. 2007, MNRAS, 382, 937

Molina, M., Bassani, L., Malizia, A., et al. 2008, MNRAS, in press, arXiv:0809.0255

Mushotzky, R. F., Baity, W. A., Peterson, L. E. 1977, ApJ, 212, 22

Ogle, P., Whysong, D., Antonucci, R. 2006, ApJ, 647, 161

Pounds, K. A., Nandra, K., Stewart, G. C., & Leighly, K. 1989, MNRAS, 240, 769

Rudnick, L., Jones, T. W., Fiedler, R. 1986, AJ, 91, 1011

Steppe, H., Salter, C. J., Chini, R., et al. 1988, A&AS, 75, 317

Tao, J., Fan, J., Qian, B., Liu, Y. 2008, AJ, 135, 737

Trussoni, E., Capetti, A., Celotti, A., et al. 2003, A&A, 403, 889

Urry, C. M. & Padovani, P. 1995, PASP, 107, 803

Wamsteker, W., Wang, T., Schartel, N., Vio, R. 1997, MNRAS, 288, 225

Wozniak, P. R., Zdziarski, A. A., Smith, D., et al. 1998, MNRAS, 299, 449

Zdziarski, A. A., Johnson, N. W., Done, C., et al. 1995, ApJ, 438, L63

Zheng, W. 1996, AJ 111, 1498